

# COMPARISON OF ELECTROMAGNETIC, THERMAL AND MECHANICAL CALCULATIONS WITH RF TEST RESULTS IN RF-DIPOLE DEFLECTING/CRABBING CAVITIES\*

H. Park<sup>1,2#</sup>, S. U. De Silva<sup>2,1</sup>, J. R. Delayen<sup>2,1</sup>,

<sup>1</sup>Thomas Jefferson National Accelerator Facility, Newport News, VA 23606, USA.

<sup>2</sup>Center for Accelerator Science, Old Dominion University, Norfolk, VA 23529, USA.

## Abstract

The current requirements of higher gradients and strict dimensional constraints in the emerging applications have required the designing of compact deflecting and crabbing rf structures. The superconducting rf-dipole cavity is one of the first novel compact designs with attractive properties such as higher gradients, higher shunt impedance and widely separated higher order modes. The recent tests performed on proof-of-principle designs of the rf-dipole geometry at 4.2 K and 2.0 K in the vertical test area at Jefferson Lab have proven the designs to achieve higher gradients with higher intrinsic quality factors and easily processed multipacting conditions. The cavity characteristics, such as pressure sensitivity and Lorentz force detuning, were studied using ANSYS before the fabrication. These characteristics were measured during the cavity test. The comparison between the simulation and the measurement provides insight how the simulation can be used for design and fabrication of future cavities.

## INTRODUCTION

The Jefferson Lab 12 GeV [1] upgrade is in need of an rf separator system that separates the maximum energy beam in to the 3 experimental halls simultaneously. Figure 1 shows the 12 GeV beam line schematic with the rf separator systems required for the energy upgrade.

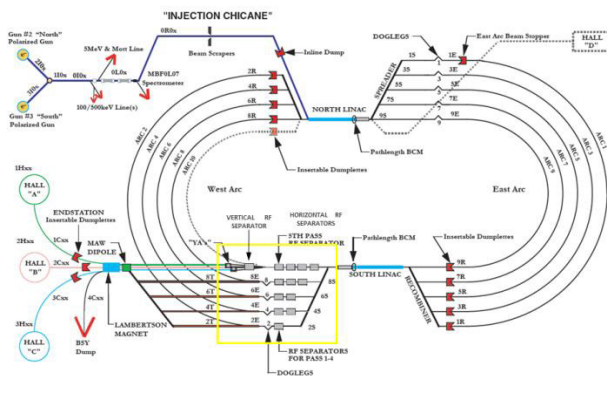


Figure 1: Jefferson Lab 12 GeV beam line.

The 6 GeV beam line has two separator systems for separating the beam horizontally and vertically. The

\*Authored by Jefferson Science Associates, LLC under U.S. DOE Contract No. DE-AC05-06OR23177. The U.S. Government retains a non-exclusive, paid-up, irrevocable, world-wide license to publish or reproduce this manuscript for U.S. Government purposes.

<sup>#</sup>hpkpark@jlab.org

horizontal separator system separates the beam that is recirculated into the linac from that sent to the experimental halls, where the vertical separator system separates the single beam into the 3 experimental halls. The existing rf separator system operates with a series of normal conducting rf separator cavities [2].

The 12 GeV energy upgrade requires a vertical rf separator system that operates at the increased beam energy. The superconducting rf-dipole cavity is one proposed options for the vertical separator system. Table 1 shows the optimized 499 MHz deflecting rf-dipole cavity [3]. The rf test results are shown in Figure 2.

Table 1: Properties of the 499 MHz Rf-dipole Deflecting Cavity

Parameter	Value	Units
Frequency	499.0	MHz
Cavity length	44	cm
Cavity diameter	25	cm
Aperture diameter ( $d$ )	40.0	mm
Deflecting voltage ( $V_T^*$ )	0.3	MV
Peak electric field ( $E_P^*$ )	2.86	MV/m
Peak magnetic field ( $B_P^*$ )	4.38	mT
Geometrical factor	105.9	$\Omega$
$[R/Q]_T$	982.5	$\Omega$
$R_T R_S$	$1.0 \times 10^5$	$\Omega^2$

At  $E_T^* = 1$  MV/m

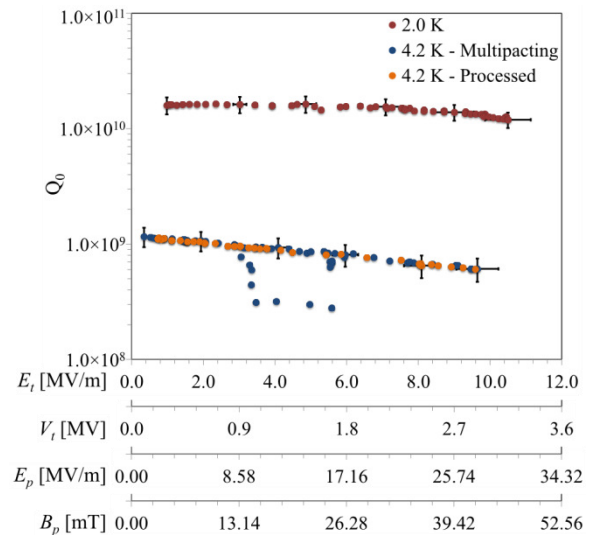


Figure 2: Q curve of the 499MHz rf dipole cavity.

### FABRICATION

The rf-dipole cavity was fabricated in parts consisting of two end caps and the center body sub-assemblies. The driving factors of the fabrication process at JLAB were the available expertise and time line. Instead of traditional stamping, machining a part of cavity was chosen due to its forming complexity and high stress identified during the study. Machining gave the freedom to increase the thickness where needed. The stiffeners were considered but not used in order to see the unstiffened cavity characteristics and performance.

Figure 3 shows the fabrication sequence. Before the electron beam welding, all parts were trimmed and chemically etched.

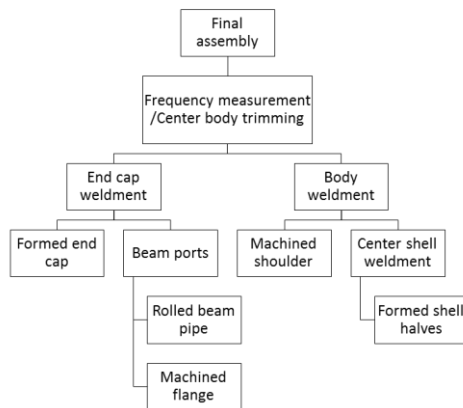


Figure 3: Fabrication sequence.

The end caps, center shell halves, and beam pipes were formed using the stamping dies. The center shell halves are open ended and they were conformed to the fixture during the longitudinal seam weld as shown in Figure 4. Figure 4 also shows the welded shell and the machined shoulder block.

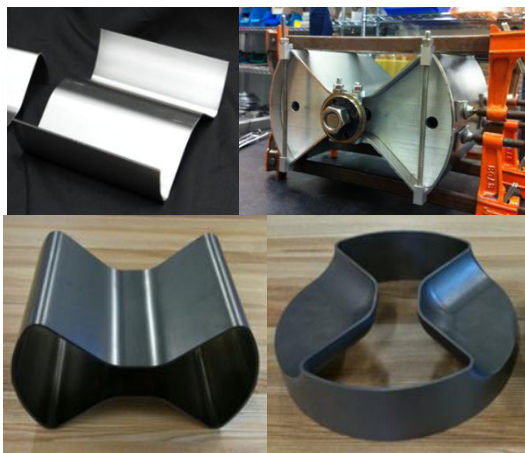


Figure 4: Formed shell halves and fixture assembly (top). Center shell weldment and shoulder block (bottom).

The sub-assemblies are then clamped tight and the frequency was measured (Figure 5). The frequency measurement and the center shell length trimming were repeated to achieve the target frequency.



Figure 5: Clamped cavity for frequency measurement.

The next weld was to assemble the center shell body to the shoulder blocks. The center shell profile was slightly mismatched to the machined shoulder which would cause the stepped transition surface when it was welded. Therefore, the two profiles were constrained again with a collapsible fixture. This fixture was inserted between the center shell and the shoulder block as shown in Figure 6. Once it was tack welded in the electron beam welding machine, the fixture was taken out and inside and outside welds were performed.



Figure 6: Weld fixturing.

The final welds were the joints between the center body sub-assembly and end cap sub-assemblies. These joints required full penetration welds from outside.

### COMPARISON

ANSYS was used for structural analyses under various conditions [4,5]. Additional analyses were conducted for predicting frequency change during the process, pressure sensitivity, Lorentz force detuning, and so on.

The target frequency of the cavity at room temperature before the final weld was calculated to be 497.8 MHz which would provide the operating frequency 499 MHz in the dewar.

Table 2 lists the cavity’s frequency change along the process. The final trimming was done anticipating 498 MHz after final welding. However the welded cavity frequency was measured much lower. The investigation concluded that the deviations in the center shell weldment from the design profile the reason. During the trimming measurement (Figure 5) the center shell gap width was smaller due to the spring back. This resulted in higher capacitance and a higher frequency. Once the shell was conformed to the design profile during the weld the gap widened which lowered the frequency.

The total frequency shift from the welded cavity at room temperature to the cooled down evacuated cavity

was calculated 0.97 MHz and the equivalent measurement was 1.01 MHz. The measurement and simulated frequency changes are in agreement.

Table 2: Frequency Changes of Cavity.

Process	Target/Simulation (MHz)	Measurement (MHz)
Before welding (clamped)	497.63	497.81
Welded cavity at room temperature	498.03	496.83
After bulk BCP	498.31	497.21
Evacuation and cool down to 4K*	499.00	497.84

\* Simulation was separate but the measurements were made at the dewar simultaneously.

The rf tests on the 499 MHz rf-dipole cavity were performed at 2.0 K and 4.2 K. The results show high unloaded quality factor and low surface resistance [6].

The pressure sensitivity during the cool down process from 4.2 K to 2.0 K was measured to be -379.5 Hz/torr. As shown in Figure 7, the simulated results give a df/dP of -255.8 Hz/torr. The difference in the pressure sensitivity could be due to difference in material properties, and non-uniformity in the fabricated cavity. The higher sensitivity can be reduced by adding stiffeners at appropriate locations.

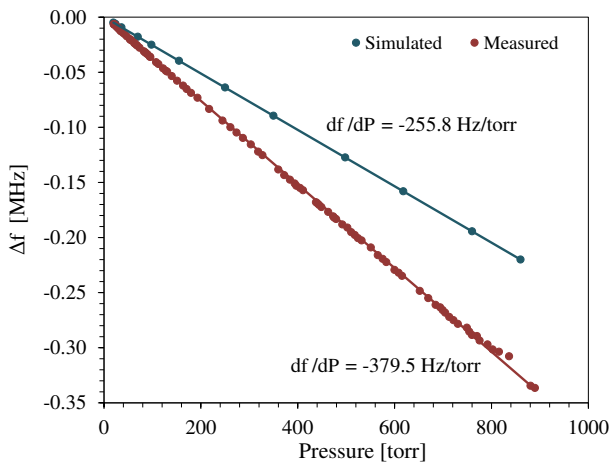


Figure 7: Pressure sensitivity of the 499 MHz rf-dipole cavity.

The Lorentz force detuning is an effect where the cavity is deformed by the radiation pressure. The magnetic field applies pressure and deforms the surface outward, while deformation due to electric field is inward. The change in cavity resonant frequency due to the deformation by Lorentz force was measured as shown in Figure 8. At 4.2 K and 2.0 K the Lorentz coefficients were calculated to be  $k_L = -57.7$  and  $-53.7$  Hz/(MV/m)<sup>2</sup>, and the slight variation in the number is possibly due to ports calibration. The simulated coefficient is  $k_L = -52.4$  Hz/(MV/m)<sup>2</sup> with a frequency shift of 5.2 kHz at a transverse voltage of 3.0 MV. This would also be reduced by adding stiffeners.

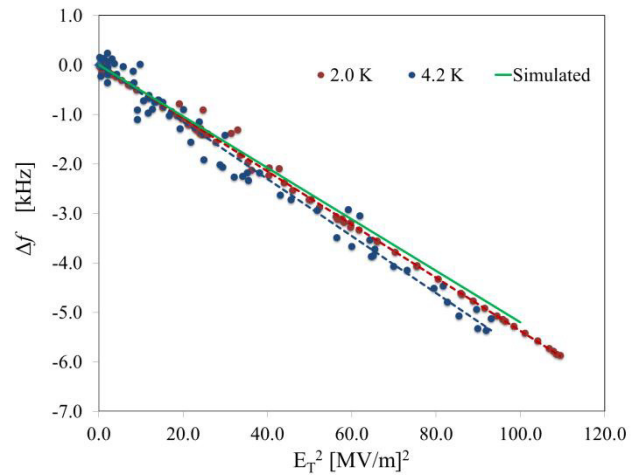


Figure 8: Lorentz force detuning at 4.2 K and 2.0 K rf tests.

## CONCLUSION

The first rf test of the 499 MHz deflecting cavity was carried out and the test results were compared with the simulations. Differences between the simulation and the actual measurements are expected due to material and fabrication tolerances. The comparison of the 499 MHz rf dipole cavity case proves that these studies are useful to predict the behavior of the cavity and help to design to minimize the adverse effects of the cavity environment. In the case of the pressure sensitivity, further study is required to understand the deviation between simulation and measurement.

## ACKNOWLEDGEMENTS

We thank Dave McCay and Casey Apeldoorn at Jefferson Lab Machine Shop for their tremendous help.

We also appreciate the support from Gary G. Cheng on the ANSYS simulation.

## REFERENCES

- [1] L. Merminga, et al., in Proceedings of the 21<sup>st</sup> Particle Accelerator Conference, Knoxville, Tennessee, Illinois (2005), p. 1482.
- [2] C. W. Leemann and C. G. Yao, in Proceedings of the Linear Accelerator Conference, Albuquerque, New Mexico, (1990) p. 232.
- [3] S. U. De Silva and J. R. Delayen, Phys. Rev. ST Accel. Beams 16, 012004 (2013).
- [4] H. Park, S. U. De Silva and J. R. Delayen, in Proceedings of 3rd International Particle Accelerator Conference, New Orleans, Louisiana (2012), p. 2450.
- [5] H. Park, J. R. Delayen and S. U. De Silva, in Proceedings of 15th Conference on RF Superconductivity, Chicago, Illinois (2012), p. 188.
- [6] S. U. De Silva and J. R. Delayen, in Proceedings of 16th Conference on RF Superconductivity, Paris, France (2013).